

Naval Research Laboratory

Washington, DC 20375-5000

②



NRL Memorandum Report 6259

DTIC FILE COPY

Segmentation of Synthetic Aperture Radar (SAR) Images of Ocean Surface by the Texture Energy Transform Method

LI-JEN DU

*Systems Control and Research Branch
Radar Division*

August 17, 1988

AD-A199 536

DTIC
ELECTE
S **D**
OCT 14 1988
E

Original contains color plates: All DTIC reproductions will be in black and white

Approved for public release; distribution unlimited.

88 10 1100

REPORT DOCUMENTATION PAGE

Form Approved
OMB No. 0704-0188

1a. REPORT SECURITY CLASSIFICATION UNCLASSIFIED			1b. RESTRICTIVE MARKINGS		
2a. SECURITY CLASSIFICATION AUTHORITY			3. DISTRIBUTION/AVAILABILITY OF REPORT Approved for public release; distribution unlimited.		
2b. DECLASSIFICATION/DOWNGRADING SCHEDULE					
4. PERFORMING ORGANIZATION REPORT NUMBER(S) NRL Memorandum Report 6259			5. MONITORING ORGANIZATION REPORT NUMBER(S)		
6a. NAME OF PERFORMING ORGANIZATION Naval Research Laboratory	6b. OFFICE SYMBOL (If applicable) Code 5380	7a. NAME OF MONITORING ORGANIZATION			
6c. ADDRESS (City, State, and ZIP Code) Washington, DC 20375-5000		7b. ADDRESS (City, State, and ZIP Code)			
8a. NAME OF FUNDING/SPONSORING ORGANIZATION Office of Naval Research	8b. OFFICE SYMBOL (If applicable) ONR	9. PROCUREMENT INSTRUMENT IDENTIFICATION NUMBER			
8c. ADDRESS (City, State, and ZIP Code) Arlington, VA 22217		10. SOURCE OF FUNDING NUMBERS			
		PROGRAM ELEMENT NO 61153N	PROJECT NO RR021- 05-43	TASK NO	WORK UNIT ACCESSION NO DN280-045
11. TITLE (Include Security Classification) Segmentation of Synthetic Aperture Radar (SAR) Images of Ocean Surface by the Texture Energy Transform Method					
12. PERSONAL AUTHOR(S) Du, Li-Jen					
13a. TYPE OF REPORT Interim	13b. TIME COVERED FROM _____ TO _____	14. DATE OF REPORT (Year, Month, Day) 1988 August 17		15. PAGE COUNT 23	
16. SUPPLEMENTARY NOTATION					
17. COSATI CODES			18. SUBJECT TERMS (Continue on reverse if necessary and identify by block number)		
FIELD	GROUP	SUB-GROUP			
			Segmentation Texture Texture transforms		
			Ocean surface Synthetic aperture radar		
19. ABSTRACT (Continue on reverse if necessary and identify by block number)					
<p>A texture energy transform approach has been chosen for the study of texture analysis and classification in digital images. It is based on the idea of detecting the degree of similarity between the spatial variation of image pixels and a set of chosen mask filters. Feature measures which characterize the texture are simpler to compute as compared with other approaches based on auto-correlation functions, digital transform methods, spatial gray tone co-occurrence probabilities, auto-regression models, etc.. An algorithm was developed for the segmentation of SAR ocean surface images into regions with and without directional streaks. Excellent results are obtained in which surface areas with relatively rough and calm water are identified.</p>					
20. DISTRIBUTION/AVAILABILITY OF ABSTRACT <input checked="" type="checkbox"/> UNCLASSIFIED/UNLIMITED <input type="checkbox"/> SAME AS RPT <input type="checkbox"/> DTIC USERS			21. ABSTRACT SECURITY CLASSIFICATION UNCLASSIFIED		
22a. NAME OF RESPONSIBLE INDIVIDUAL Li-Jen Du			22b. TELEPHONE (Include Area Code) (202) 367-2000 FACSIMILE (202) 367-2000 Code 5380		

CONTENTS

INTRODUCTION	1
TEXTURE ENERGY TRANSFORM APPROACH	2
EXPERIMENTAL METHODS	5
EXPERIMENTAL RESULTS AND DISCUSSIONS	10
CONCLUSIONS	21
REFERENCES	23

Accession For		
NTIS GRA&I	<input checked="" type="checkbox"/>	
DTIC TAB	<input type="checkbox"/>	
Unannounced	<input type="checkbox"/>	
Justification		
By		
Distribution/		
Availability Codes		
Dist	Avail and/or	Special
A-1		



*Original contains color
plates: All DTIC reproductions
will be in black and
white*

SEGMENTATION OF SYNTHETIC APERTURE RADAR (SAR) IMAGES OF OCEAN SURFACE BY THE TEXTURE ENERGY TRANSFORM METHOD

Introduction

Texture analysis is an important aspect of image classification and segmentation tasks. It is fundamental to some applications such as metal surface analysis, radiographic diagnosis, identification of different terrains in aerial photographs, isolating special regions in natural scenes, etc.. The subject has been studied quite extensively [1]. Different statistical approaches have been employed to evaluate quantitative feature measures from image pixel data for texture characterization. Despite the ingenious ideas used and the success accomplished in classifying the images chosen in the previous researches, most texture analysis approaches still have limitations. They were applied to a limited categories of images and may not work well in general. All of them require tedious time-consuming machine processing.

Recently, Laws [2] introduced a different kind of approach to texture measures which he called the texture energy transform. In this approach, texture features are evaluated in a spatial-statistical sequence of small mask convolutions followed by moving

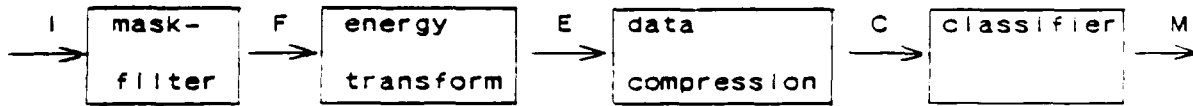
window averaging. The results are closely related to the degree of match between the pixel neighbourhoods and the set of chosen masks. In addition to possessing an intuitive physical reasoning in the formulation, these features are also simpler to compute. Application of this approach to texture classification yielded better results than other standard techniques based on second order gray level statistics [2,3]. It can also be made invariant to changes in luminance, contrast, and rotation without the use of histogram equalization or other preprocessing.

In this report, we present the results of texture segmentation of SAR images of ocean surface using this new technique. It is a continuation of the task reported previously where similar images were classified by the gray-tone co-occurrence matrix approach [4]. The previous results obtained are not as good as we had hoped for which prompted the search for a different processing method. Our objective of mapping the image into two kinds of regions differentiated by the presence and absence of pixel streak patterns has been successful. Physically speaking, this separation process identifies the areas of ocean surface where significant difference existed in terms of surface wind patterns and wave structures.

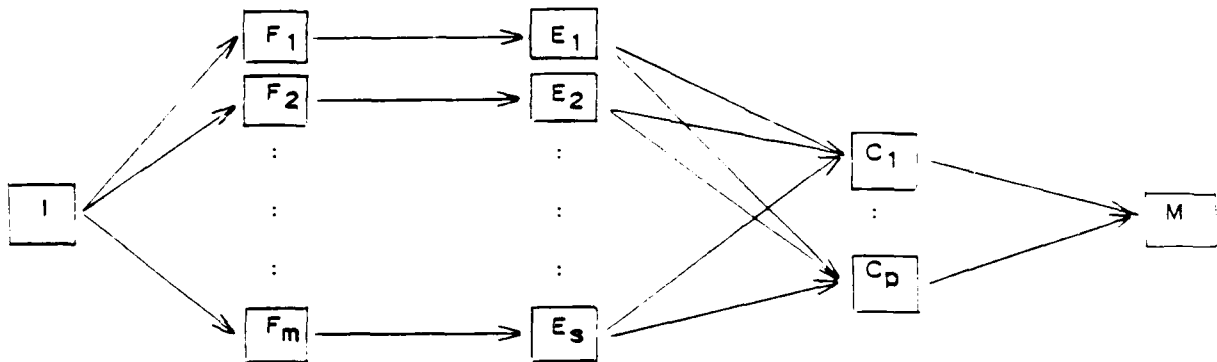
Texture Energy Transform Approach

The processing sequence of the texture energy transform approach to image segmentation is outlined in Figure 1. The operation steps involved are shown in the upper part of the figure with the associated frames of data attached below. A more detailed

description of the first two steps is shown in Figure 2.



(a) Operation sequence



(b) Image frame sequence

Fig. 1. Texture energy transform approach.

The original image, I , is first filtered by a set of micro-filter convolution masks with integer elements to generate the set of F plane images. The pixel data in an F plane image is a function of the original image and the chosen filter. They can assume negative as well as positive values. These filtered images are plane frames of data in the processing sequence and may not represent recognizable images. The filtered F plane images are then processed by evaluating statistics of data within a scanning macro-window and assigning the result to the center pixel to produce the E plane

Images. This is a continuous region-to-point transformation

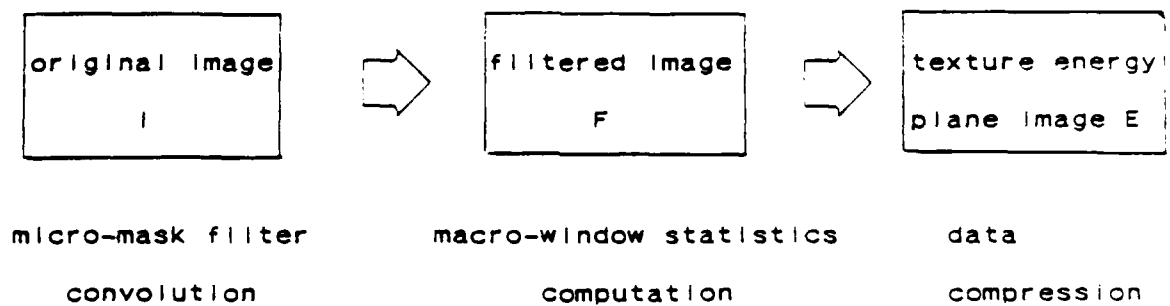


Fig. 2. Spatial-statistical processing sequence.

where a pixel in a E plane image acquires a number descriptive of its immediate neighbourhood in the original image. The size of the convolution mask is chosen to be comparable to that of the typical texture primitives of the original image. The macro-window should have a size appropriate to cover one kind of texture region most of the time and two kinds of regions along the boundary of region separation. It is chosen so that the statistics evaluated will reveal the difference when it is located within different regions. These statistics are more representative of local spatial variations than typical frequency domain measures and are suitable for textures with short coherence length or correlation distance. To reduce the required processing time, the dimensions of masks and windows are chosen sufficiently small to be physically reasonable for the images under study.

If there are many E plane images chosen, an optional step may be

taken to compress them into a small number of principal component C plane images which still carry enough discriminating information. This can be achieved by using the Hotelling transform which picks out the orthogonal image components with the largest variance [5].

The texture energy plane images or the principal component plane images are the input to the classifier which assign each pixel the proper texture label to produce the final segmented image M. Classification is simple if texture classes are known and training samples are available. Clustering and segmentation algorithms must be used in addition to that of the classification algorithm if texture classes are unknown and have to be identified.

Experimental Methods

In the first step of the texture processing, the original image is filtered by a set of convolution masks. These masks are constructed as two dimensional matrix multiplication of the linear masks shown in Figure 3. These linear masks are called Lattice Aperture Waveform Sets of order three, five and seven. The names of the vectors are mnemonics for level, edge, spot, wave, ripple, undulation, and oscillation. All of them are symmetrically weighted toward their center. Except for the level vectors, the sum of all the elements in each equates to zero. Linear vectors of length three form the basis since the longer ones can be derived in terms of these three through repeated linear convolution.

Figure 4 shows the nine square filter masks generated by the

three linear vectors of length three. Any 3 by 3 mask can be

$$\begin{aligned}L3 &= (1, 2, 1) \\E3 &= (-1, 0, 1) \\S3 &= (-1, 2, -1) \\L5 &= (1, 4, 6, 4, 1) \\S5 &= (-1, 0, 2, 0, -1) \\R5 &= (1, -4, 6, -4, 1) \\E5 &= (-1, -2, 0, 2, 1) \\W5 &= (-1, 2, 0, -2, 1) \\L7 &= (1, 6, 15, 20, 15, 6, 1) \\E7 &= (-1, -4, -5, 0, 5, 4, 1) \\S7 &= (-1, -2, 1, 4, 1, -2, -1) \\W7 &= (-1, 0, 3, 0, -3, 0, 1) \\R7 &= (1, -2, -1, 4, -1, -2, 1) \\O7 &= (-1, 6, -15, 20, -15, 6, -1)\end{aligned}$$

Fig. 3. Center-weighted mask filters.

expressed as a unique linear combination of them. The names of these masks attached underneath are coined by the names of the two linear vectors constituting the column and row vectors of the corresponding matrix of the mask. 5 by 5 and 7 by 7 as well as non-square rectangular masks can be formed in a similar fashion. Figure 5 shows four 5 by 5 masks which were found to be most useful in the experimental work done by Laws [2]. The structure of these masks as the matrix product of the elements in the basis set helps to simplify the algorithm and reduce the computation time in the step of

convolution filter processing.

$\begin{vmatrix} 1 & 2 & 1 \\ 2 & 4 & 2 \\ 1 & 2 & 1 \end{vmatrix}$	$\begin{vmatrix} -1 & 0 & 1 \\ -2 & 0 & 2 \\ -1 & 0 & 1 \end{vmatrix}$	$\begin{vmatrix} -1 & 2 & -1 \\ -2 & 4 & -2 \\ -1 & 2 & -1 \end{vmatrix}$
L3L3	L3E3	L3S3
$\begin{vmatrix} -1 & -2 & -1 \\ 0 & 0 & 0 \\ 1 & 2 & 1 \end{vmatrix}$	$\begin{vmatrix} 1 & 0 & -1 \\ 0 & 0 & 0 \\ -1 & 0 & 1 \end{vmatrix}$	$\begin{vmatrix} 1 & -2 & 1 \\ 0 & 0 & 0 \\ -1 & 2 & -1 \end{vmatrix}$
E3L3	E3E3	E3S3
$\begin{vmatrix} -1 & -2 & -1 \\ 2 & 4 & 2 \\ -1 & -2 & -1 \end{vmatrix}$	$\begin{vmatrix} 1 & 0 & -1 \\ -2 & 0 & 2 \\ 1 & 0 & -1 \end{vmatrix}$	$\begin{vmatrix} 1 & -2 & 1 \\ -2 & 4 & -2 \\ 1 & -2 & 1 \end{vmatrix}$
S3L3	S3E3	S3S3

Fig. 4. 3 by 3 center-weighted mask filters.

Each mask filter has a unique combination of elements. Convolution will produce a plane of positive or negative numbers of larger magnitude if the spatial pixel data variation of the original image, I , matches closely that of the mask. A homogeneous image region which shows no textural structure, or a textural region whose spatial structure differs from that of the mask will result in smaller numbers. The data in the F plane image reveals the degree of textural similarity between the mask and the corresponding immediate vicinity in image I . Pixels located within different textural

primitives in image I will have numerical values of different levels in plane. Hence, the transformation from I to F provides a

-1	-4	-6	-4	-1	1	-4	6	-4	1
-2	-8	-12	-8	-2	-4	16	-24	16	-4
0	0	0	0	0	6	-24	36	-24	6
2	8	12	8	2	-4	16	-24	16	-4
1	4	6	4	1	1	-4	6	-4	1
E5L5					R5R5				
-1	0	2	0	-1	-1	0	2	0	-1
-2	0	4	0	-2	-4	0	8	0	-4
0	0	0	0	0	-6	0	12	0	-6
2	0	-4	0	2	-4	0	8	0	-4
1	0	-2	0	1	-1	0	2	0	-1
E5S5					L5S5				

Fig. 5. 5 by 5 center-weighted mask filters.

separation step among different texture primitives. The pattern and the steepness in separation among the texture primitives vary among the different masks.

Familiar statistics such as mean, variance, standard deviation, range, maximum, minimum, skewness, kurtosis, and etc. can be chosen as the texture feature representation in the macro-window processing of F plane images to generate E plane images. Laws concluded in his study that variance or standard deviation alone is sufficient in extracting the necessary information. If all mask filters chosen in

the convolution process have zero sum elements, the F plane image is essentially a zero mean pixel field. Variance is an average of squared deviation from the mean. With a vanishing mean value, the variance becomes the average of the squared pixel values within the macro-window. In this sense, each pixel's value in E plane image is an energy measure of its macro-window neighbourhood in the F plane. To simplify the calculation and still maintain essentially the same statistical meaning, the average of the absolute values within the macro-window was chosen as the statistic and its value is assigned to the center pixel of the window in the E plane image.

For each selection of the mask and statistic combination, there is one feature measure of the texture. Since the choice of the statistic is a fixed one, the number of masks chosen determines the number of features to be computed and the number of E plane images to be generated. The discriminating power of a feature is judged by the F-ratio statistic calculated from the available training sample image data by the following formula from [8],

$$F = \frac{\text{variance of inter-class sample means}}{\text{combined intra-class variance}}$$

A good choice of feature will generate values with small variance from texture samples of the same type and significantly different mean values of samples of different types. Better choices of features will produce higher F-ratio statistics. The statistical meaning of the F-ratio also depends upon the number of the samples involved. The comparison of these ratios has to be made on equal

number of samples to yield accurate judgement. With many choices of features available for characterization of differences among the textural categories, the proper combination of them to generate the best accuracy of discrimination can be obtained through discriminant analysis under certain statistical criteria [2,7]. In the procedure of segmenting an image, the feature vector composed of chosen feature elements evaluated for each pixel's neighbourhood is compared with the feature vectors evaluated by the same formulas from known training samples of each class. A pixel is classified as belonging to the class whose centroid vector has the least distance separation from the feature vector evaluated in its vicinity.

Experimental Results and Discussions

Figures 6a, 7a, and 8a show the images which we wish to segment using the texture energy transform method. These are sub-images obtained during the SIR-B mission on October 11, 1984. Each one has a size of 512 by 512 pixels. The area covered is outside the U.S. east coast with the center geographic location around 37 degree north and 74 degree west. By carefully examining these images, we can realize that there are two kinds of textures present. First, the pixel variations indicate directional streak patterns. In other kind of texture, the pixel variation seems homogeneously random. The appearance of these two textures indicates the difference in the radar back-scattering characteristics from different areas of ocean surface. Our image segmentation objective is to separate these two textural areas where contrasting surface meteorological conditions existed when the image was recorded.

According to Laws' research, 5 by 5 masks were more powerful than the 3 by 3 masks, and much simpler to process than 7 by 7 masks. By detailed comparison, we found that the 5 by 5 mask is big enough to cover an essential part of a typical texture primitive in these images. We chose to try the masks shown in Figure 5 first. Four training samples with size of 64 by 64 pixels of streak areas and non-streak areas were located in each image.

Since there are only two classes of texture to be separated, the complicated discriminant analysis is not necessary in this problem. Each five by five mask was convolved with each of the training samples and the average of absolute values of the convolution was then computed. There are small differences between these two kinds of textures and the results are not much better than what had been achieved using the co-occurrence matrix method [4]. However, mask filters E5L5 and L5S5 did produce consistently more difference than the other two filters. E5L5 is a horizontal edge mask and L5S5 is a vertical line detector. This fact indicates that the edge and line detector masks can separate image regions with streaks and without streaks more effectively than masks which discover textural detail in other aspects. Attention was shifted toward finding the best possible line detector masks which are zero-sum and made of simple integer components. Judgement was made on tests done with the training samples of each image. The most powerful masks found this way are shown in Figures 9, 10, and 11 for the images in Figures 6a, 7a, and 8a respectively. The two masks shown in each figure are a 90 degree transpose of each other. One of

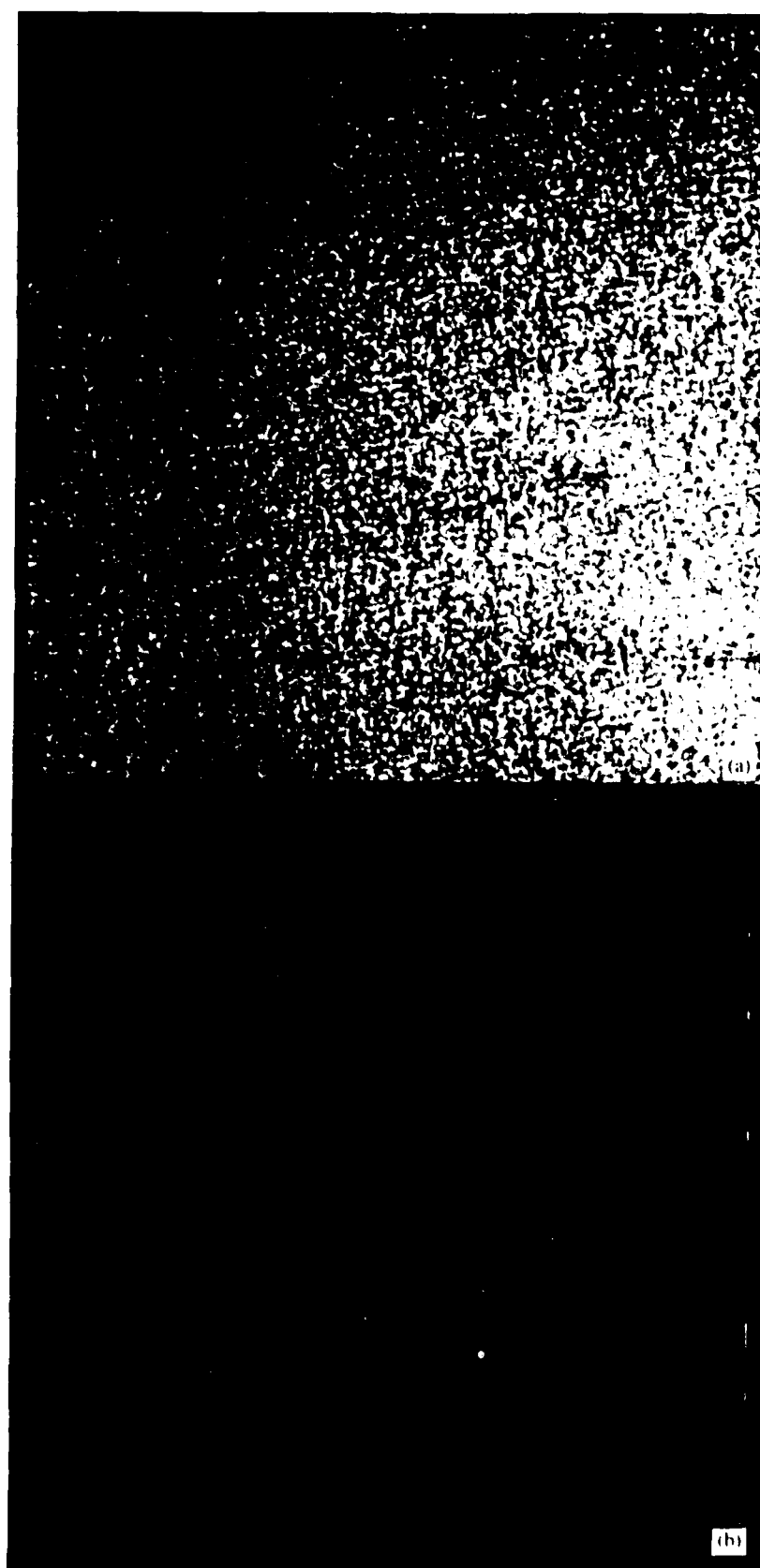


Fig. 6. SAR ocean surface image and its segmentation map.

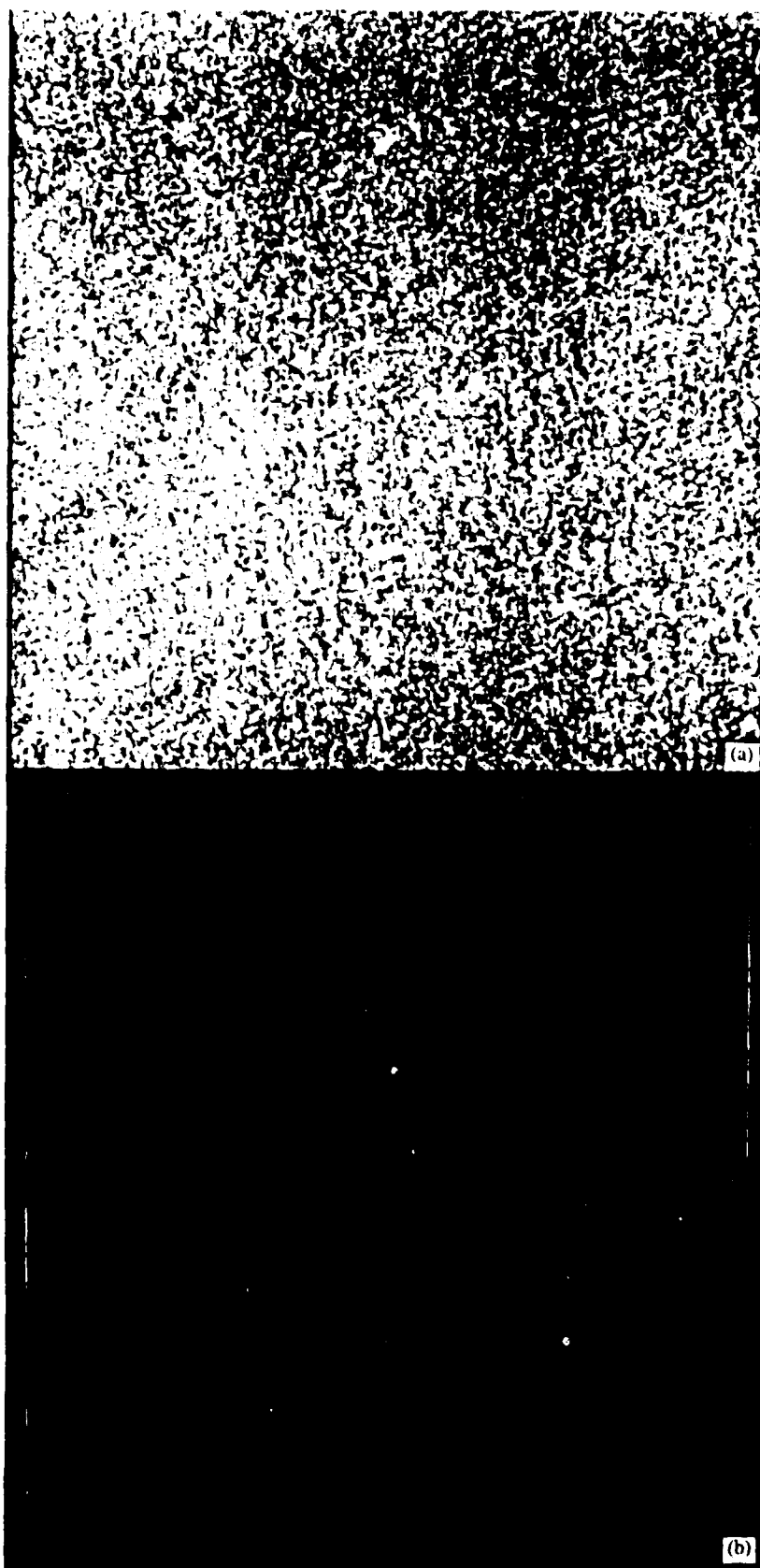


Fig. 7. SA ocean surface image and its segmentation map.

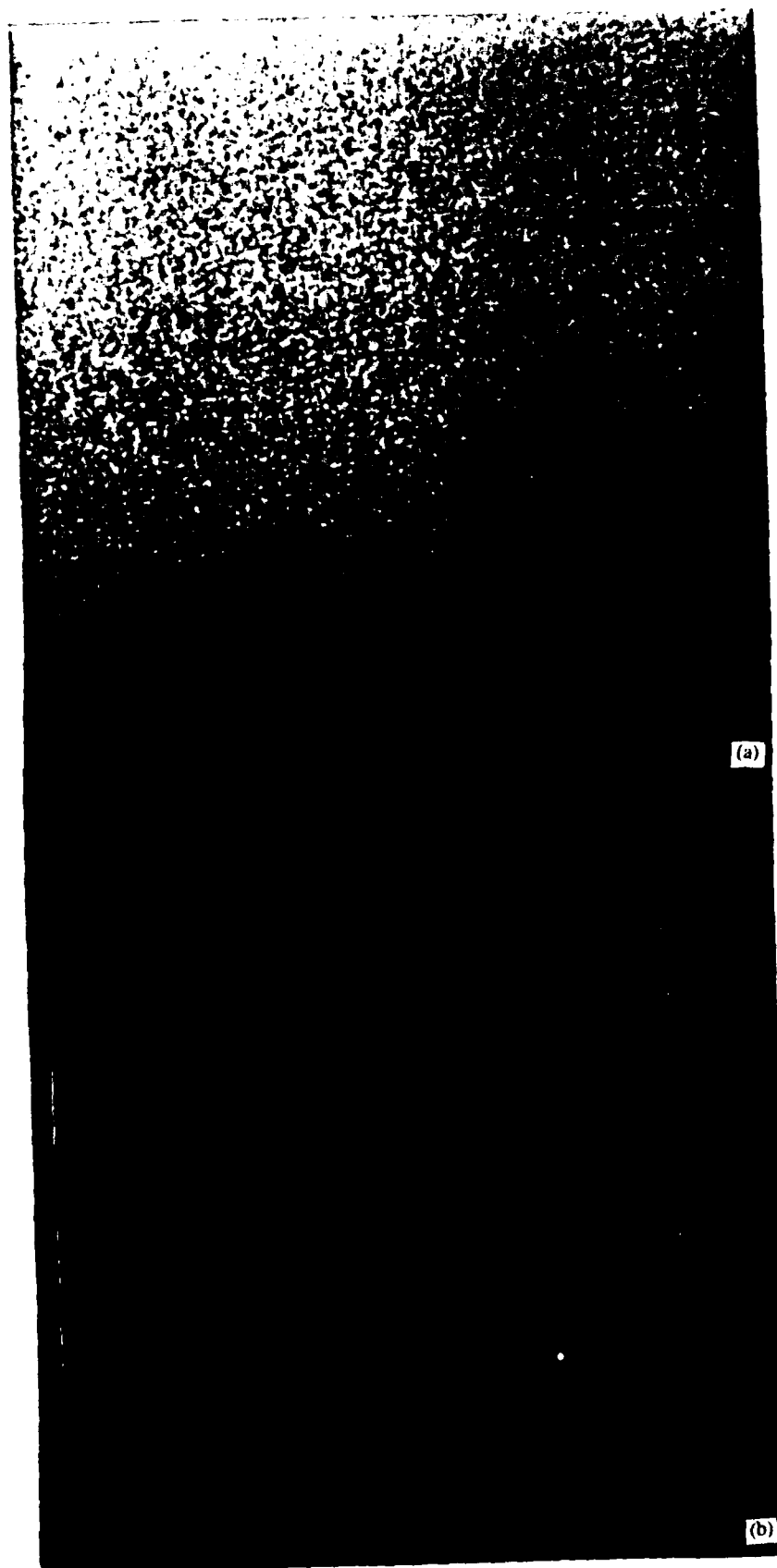


Fig. 8. SAR ocean surface image and its segmentation map.

-11	-2	0	2	11	-11	-11	-11	-11	-11
-11	-2	0	2	11	-2	-2	-2	-2	-2
-11	-2	0	2	11	0	0	0	0	0
-11	-2	0	2	11	2	2	2	2	2
-11	-2	0	2	11	11	11	11	11	11

Fig. 9. Mask filter chosen for image in Fig. 6a.

-2	-1	0	1	2	-2	-2	-2	-2	-2
-2	-1	0	1	2	-1	-1	-1	-1	-1
-2	-1	0	1	2	0	0	0	0	0
-2	-1	0	1	2	1	1	1	1	1
-2	-1	0	1	2	2	2	2	2	2

Fig. 10. Mask filter chosen for image in Fig. 7a.

-5	-4	0	4	5	-5	-5	-5	-5	-5
-5	-4	0	4	5	-4	-4	-4	-4	-4
-5	-4	0	4	5	0	0	0	0	0
-5	-4	0	4	5	4	4	4	4	4
-5	-4	0	4	5	5	5	5	5	5

Fig. 11. Mask filter chosen for image in Fig. 8a.

them detects the vertical lines and edges and the other detects the horizontal counterparts. Both were utilized simultaneously as the direction of the streaks can be random. Applying these pairs of filters to the corresponding training samples and taking the sum of the two average absolute values in each case yields two-point scatter plots. Two threshold levels for each image to separate the streak and non-streak textures as well as a transition region were

determined. Static threshold levels chosen this way were incorporated into the process to classify the corresponding whole image.

Starting at the upper left corner, the mask filters in Figures 9, 10, and 11 were scanned pixel by pixel to compute convolution through the whole image. A moving macro-window of size 33 by 33 pixels was chosen so that there is a precisely defined center location. The macro-window is also scanned pixel by pixel through the image. At each position in the scanning process, the sum of the average absolute values of the convolutional results of the two perpendicular masks within the window was taken. This sum is then adjusted to eliminate the influence due to the difference in the mean pixel value within the window at each position in the original image. This adjusted sum is compared with the two threshold levels to determine the center pixel's classification. Segmentation results are shown in Figures 6b, 7b, and 8b for the images in Figures 6a, 7a, and 8a respectively. Pseudo colors are used for clarification. Green color is assigned to the streak textural regions and the blue color is assigned to the non-streak textural regions. The transition regions are cyan. Sixteen pixels around the edge could not be classified and are colored red. The threshold levels are adjustable. The threshold level chosen for streaked regions of Figure 6 was more stringent. As a consequence, less area was classified as streaked region in Figure 6 as compared to those in the other two images. The lower left corner of Figure 6 was not accurately classified because the original pixel data there was incomplete. The size of the macro-window can be varied, but its optimum size may not be easy to find.

In some parts of these images the perception does change somewhat as the window size varies or as the average pixel intensity within the window varies. However, careful scrutiny of the corresponding images shows that these results do present accurate maps which separate the two kinds of textures.

Conclusions

The texture energy transform is the latest method developed for texture analysis of images. It is based on a spatial-statistical approach in which texture features are determined by the degree of match between pixel neighbourhood of the image and a set of chosen mask filters. The method is conceptually simple and consumes less computation time than most other established texture classification techniques. It was applied to segmentation of synthetic aperture radar (SAR) images of ocean surface into regions with and without directional streaks. Excellent results were obtained. However, the set of masks incorporated in the analysis, which worked well, are masks detecting lines and edges rather than the standard set originally proposed to discover essentially all possible spatial variations. This fact indicates that the textural difference between the regions with and without streaks are subtler than we anticipated. The distinction can be recognized without much difficulty with naked eyes but it may not be easy to establish by algorithms based on various conventional texture discriminating methods. Since both the co-occurrence matrix method and the texture energy transform method produced the same level of difference in feature measures between the two kinds of the training samples, we believe they are almost equally

powerful in texture analysis. For the SAR ocean surface images we tried to segment, it appears more efficient to search for the existence of lines or edges rather than for two different kinds of textures. It is unlikely that any other powerful texture analysis method will be able to discern these two regions in terms of clear cut texture dissimilarity.

The size of the micro-filter masks and the macro-window for texture energy evaluation are determined individually for each task under investigation to match the intrinsic spatial texture variations and each textural region's typical extent of coverage. The masks suggested by Laws [2] cover a very general case in which many kinds of drastically different textures are involved. Laws masks are derived by a two dimensional matrix multiplication of two linear vectors which are obtained from sequence of convolutions with three vectors of length three. Choice of these masks can simplify the mask convolution calculation and save processing time. The optimum combination of masks which make the set for the feature vector components can be determined through F-ratio statistic test and discriminant analysis with the training samples. For simpler problems with fewer classes of textures to segment, like the one studied in this report, one or two feature measures which yield clearly different range of values among different classes may be enough and the F-ratio test is not necessary. Proper workable masks can be found by trial and error and the textural identification can be done with threshold level separation instead of the complicated statistical classifications.

References

- [1] Robert M. Haralick, "Statistical and Structural Approaches to Texture," Proceedings of the IEEE, vol. 67, no. 5, pp.786-804, 1979.
- [2] Kenneth I. Laws, "Textured Image Segmentation," Image Processing Institute, University of Southern California, Report 940, Jan. 1980.
- [3] Matti Pietikainen, Azriel Rosenfeld, and Larry S. Davis, "Experiments with Texture Classification Using Averages of Local Pattern Matches," IEEE Trans. Systems, Man, and Cybernetics, vol. SMC-13, no. 3, pp. 421-426, 1983.
- [4] L. Du, "Texture Study of Synthetic Aperture Radar(SAR) Images of Ocean Surfaces," Naval Research Laboratory, Memorandum Report 6005, September 1987.
- [5] Rafael C. Gonzalez and Paul Wintz, Digital Image Processing. Reading, Massachusetts: Addison-Wesley, 1977.
- [6] Lyman Ott, An Introduction to Statistical Methods and Data Analysis. Boston, Massachusetts: Duxbury Press, 1984.
- [7] M. J. Norusis, SPSS Statistical Algorithms Release 8.0. Chicago:SPSS Inc., 1979.